

Contrastive Spatial Reasoning on Multi-View Line Drawings

Siyuan Xiang^{*‡} Anbang Yang^{*‡} Yanfei Xue[‡] Yaoqing Yang[§] Chen Feng^{†‡}

[‡]New York University Tandon School of Engineering [§]University of California, Berkeley

<https://ai4ce.github.io/Contrastive-SPARE3D/>

Abstract

Spatial reasoning on multi-view line drawings by state-of-the-art supervised deep networks is recently shown with puzzling low performances on the SPARE3D dataset. To study the reason behind the low performance and to further our understandings of these tasks, we design controlled experiments on both input data and network designs. Guided by the hindsight from these experiment results, we propose a simple contrastive learning approach along with other network modifications to improve the baseline performance. Our approach uses a self-supervised binary classification network to compare the line drawing differences between various views of any two similar 3D objects. It enables deep networks to effectively learn detail-sensitive yet view-invariant line drawing representations of 3D objects. Experiments show that our method could significantly increase the baseline performance in SPARE3D, while some popular self-supervised learning methods cannot.

1. Introduction

Human visual reasoning, especially spatial reasoning, has been studied from psychological and educational perspectives [17, 20]. Trained humans can achieve good performance on spatial reasoning tasks [32], because they can solve these tasks with spatial memory, logic, and imagination. However, the spatial reasoning ability of deep networks is yet to be explored and improved. For other visual learning tasks such as image classification, object detection, or segmentation, deep networks might perform superior to human by memorizing the indicative visual patterns from various image instances for prediction. However, it seems difficult for deep networks to reason in the same way about the spatial information such as the view consistency and camera poses from 2D images [13].

In this paper, we investigate the SPARE3D¹ dataset [13], which provides several challenging spatial reasoning tasks

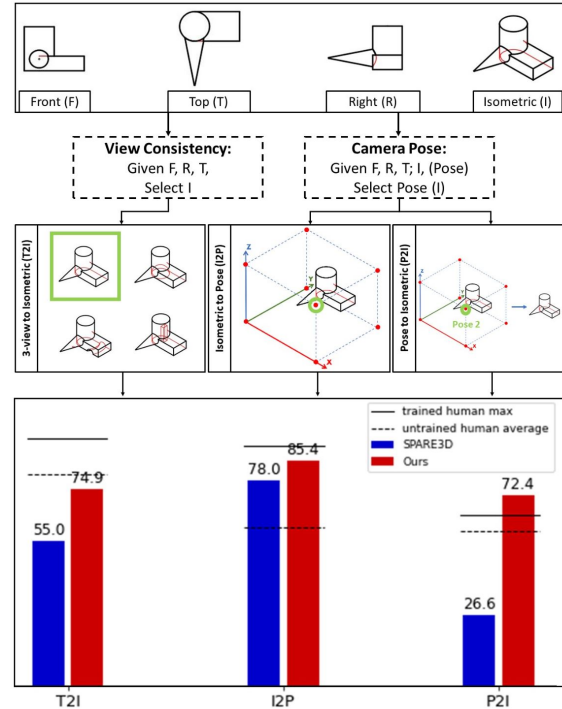


Figure 1. We significantly improves SPARE3D baselines, especially on the *T2I* task using our contrastive spatial reasoning.

on line drawings (Figure 1). Specifically, we focus on the view-consistency reasoning task (the Three-view to Isometric or *T2I*) and the two camera-pose reasoning tasks (the Isometric to Pose or *I2P*, and the Pose to Isometric or *P2I*). The view-consistency reasoning task requires a deep network to select the correct isometric view drawing out of four visually similar candidates that are consistent with the three-view (front, right, and top views) drawings given in the question. For the camera-pose reasoning tasks, given three-view drawings, the network is asked to determine the camera pose of a given isometric drawing or select the correct isometric drawing from a given viewing pose.

So “why is the baseline performance on SPARE3D low”? This important question is raised in [13] with three conjectures: 1) the dataset is non-categorical, 2) the images are line drawings, and 3) spatial reasoning is not image re-

^{*}Equal contribution.

[†]The corresponding author is Chen Feng cfeng@nyu.edu.

¹Note that we use the latest dataset and benchmark results updated by the SPARE3D authors after CVPR 2020.

trieval. The first two conjectures inspire us to first understand the task characteristics, and study the factors that affect the network’s performance on those tasks, which leads to our quantitative investigations about a network’s ability on the SPARE3D tasks using controlled experiments.

The last conjecture is related to the intuitive difference between reasoning and other discriminative learning tasks. Bengio [4] pointed out that reasoning can be considered as *Kahneman’s system 2* problem [19], which “requires a sequence of conscious steps”, and is slower, more deliberative, and more logical compared to system 1 problems that are “fast, instinctive and emotional”. This inspires us to rethink the SPARE3D baselines’ training mechanism, which is fully supervised. Although there seems to have no consensus yet on how to extend deep networks from system 1 to system 2, we find self-supervised learning, especially contrastive learning, a promising mechanism to improve the baseline SPARE3D performances, due to its similarity to how humans intuitively learn to solve SPARE3D tasks. Compared to supervised learning, self-supervised learning is helpful when a large amount of unlabeled data are available. Moreover, in many visual learning tasks, self-supervised learning as a pre-training task learns better visual representations, which can be further fine-tuned via supervision for downstream tasks, achieving similar or even better results than supervised learning [7].

Based on the above analysis, we design a contrastive spatial reasoning method specialized to tackle the challenges in SPARE3D tasks (Figure 5). This is necessary and non-trivial because few existing contrastive learning methods consider explicitly the relationship between different views, nor do they force deep networks to focus on detailed differences between images. Contrarily, we demonstrate both qualitatively and quantitatively that *our method helps deep networks to capture these small details while being view invariant*, which is crucial for the view consistency task.

In sum, our major contributions are:

- A novel contrastive learning method by self-supervised binary classifications, which enables deep networks to effectively learn detail-sensitive yet view-invariant multi-view line drawing representations;
- Extensive controlled experiments to improve our empirical understandings of SPARE3D tasks, which further help us improve network design for these tasks;
- Significantly improved spatial reasoning performance of deep networks on line drawings based on the above, some of which surpass the human baselines.

2. Related Work

Self-supervised learning has achieved great success due to the performance improvement on many visual learning tasks [12, 22, 27, 39]. Successful self-supervised learning should have proper artificial labels designed from the input image itself. One way is to use spatial information or spa-

tial relationships between image patches in a single image. For example, Gidaris et al. [11] designed the pretext task by asking the network to predict image rotations. Another way is to ask the network to recover the positions of shuffled image patches [21, 29, 40], or predict the relative position [9]. In addition, color signal contained in an RGB image could also be used. By recovering the color for grayscale images generated from RGB images, networks can learn the semantic information of each pixel [24, 44]. Despite the success, for the spatial reasoning tasks in the SPARE3D dataset, we expect these methods to be insufficient since they only use the visual information from a single image. Methods considering the common information between different images could be more suitable to solve those reasoning problems.

Contrastive learning. One way of grouping various self-supervised learning methods is to divide them into generative vs. contrastive ones [26]. On the one hand, generative ones learn visual representations via pixel-wise loss computation and thus forcing a network to focus on pixel-based details; on the other hand, contrastive ones learn visual representations by contrasting the positive and negative pairs [1]. Next, we briefly review some contrastive learning methods to help common visual learning tasks.

Many researchers explored contrastive learning by comparing shared information between multiple positive or negative image pairs. These methods all try to minimize the distance of the features extracted from the same source data, and maximize the distance between features from different source data in the feature space. Hjelm et al. [16] propose Deep InfoMax based on the idea that the global feature extracted from an image should be similar to the same image’s local feature and should be different from a different image’s local feature. Based on this method, Bachman et al. [3] further use image features extracted from different layers to compose more negative or positive image pairs. SimCLR [6] differs from the previous two methods in that it only considers the global features of the augmented image pairs to compose positive and negative pairs. SimCLRv2 [7] make further improvements on Imagenet [8] by conducting contrastive learning with a large network, fine-tuning using labeled data, and finally distilling the network to a smaller network. Compared to SimCLR, MoCo [14] stores all generated samples to a dictionary and uses them as negative pairs, instead of generating negative pairs in each step. These tactics could help reduce the batch size requirement while still achieve good performance. Differently, SwaV [5] trains two networks that can interact and learn from each other, with one network’s input being the augmented pair of another network’s input. Besides, researchers also theoretically analyze why these contrastive learning methods work well [2, 25, 37, 38].

However, *it is difficult to apply the aforementioned contrastive learning methods directly to tasks which requires*

consideration of the relationships between multi-view images. Contrastive multiview coding [36] has a misleading name in our context because that “multiview” in fact means different input representations instead of views from different camera poses. Therefore it is not suitable for SPARE3D tasks. Kim et al. [23] propose a method to solve a few-shot visual reasoning problem on RAVEN dataset [43], which is perhaps more relevant to us due to the use of contrastive learning in visual reasoning. Yet because it is designed for analogical instead of spatial reasoning, it is not directly applicable to SPARE3D tasks either.

Controlled experiments on deep learning. There is a branch of research that investigates how data and networks affect deep visual learning performance via controlled experiments. Funke et al. [10] found that using ImageNet pre-trained network parameters for initialization could significantly improve performances on other visual tasks that seem to have a big domain gap with ImageNet, which inspires us to check whether the same approach is effective for SPARE3D tasks because of the similar domain gap. Moreover, we study the network’s capacity and structure for SPARE3D tasks, inspired by [15, 18, 35, 42].

3. What Affects SPARE3D Performance?

To better understand the SPARE3D tasks and why state-of-the-art deep networks have low performances, we study three potentially relevant factors: *CAD model complexity*, *network capacity*, and *network structure* respectively. For each factor, we first give a natural hypothesis about its influence on SPARE3D baseline performance. Then, we design controlled experiments to prove or disprove the hypothesis, and finally obtain heuristics about both the causes of existing baseline’s low performance and potentially more effective network designs.

Controlled experiment settings. For investigating the *CAD model complexity* and the *network capacity* factors, we focus on the view-consistency reasoning (*T2I*) and the camera-pose reasoning (*I2P*) tasks on SPARE3D-ABC dataset. For the *network structure* factor, we use both the *T2I*, the *I2P*, and the *P2I* tasks. We follow the same baseline settings as in [13]: for *T2I* and *P2I* tasks, we use the *binary classification* baseline networks; for *I2P* task, we use the *multi-class classification* baseline network. The backbone network for these baseline networks are VGG-16 [34]. We select these baseline networks since they are the best performing ones in [13]. All experiments are implemented using PyTorch [30] and conducted on NVIDIA GeForce GTX 1080 Ti GPU. For each experiment, we tune the hyperparameters to seek the best performance (details in the supplementary material).

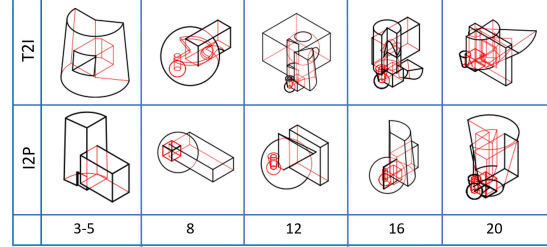


Figure 2. CSG models with different number of primitives.

3.1. CAD model complexity

Motivation: we want to study if the level of CAD model complexity affects the baseline performance for SPARE3D tasks. It is discussed in [28] that the complexity of a CAD task is associated with its difficulty for humans. However, the relationship between the CAD model complexity and the difficulty level for deep networks to solve the spatial reasoning tasks has not been fully studied. To study the influence of CAD model complexity for deep networks, we use the number of primitives in CAD models to represent the complexity of CAD models, as discussed in [28]. In practice, we use the constructive solid geometry (CSG) modeling method to generate the dataset with different numbers of primitives yet fixed primitive types and boolean operations. With the increasing number of primitives of the CSG models, the level of CAD complexity also increases.

Hypothesis 1: *the higher level of CAD model complexity will cause lower SPARE3D baseline network performance, as long as the corresponding line drawings are still visually legible for the reasoning tasks.*

Experiment details. We use FreeCAD [33] to generate CSG model dataset with a various number of primitives. We follow the generation settings as in [13]. The primitives used are sphere, cube, cone, and cylinder; the Boolean operations used are intersection, union, and difference. For both the task *T2I* and *I2P*, we generate seven groups of CSG models, with primitive number 3-5, 8, 12, 16, 20, 24, and 30. The 3-5 means the number of primitives making up a CAD model is 3, 4, or 5. For each group, it has 4000 models for training and 500 models for testing. Exemplar line drawings rendered with CAD models composed of the different number of primitives can be seen in Figure 2. We can see that the models become visually more complex when the number of primitives increases.

Experiment results. Figure 3 left shows that for the *T2I* task, in general, the more primitives a CSG model has, the lower the testing accuracy is, as expected in Hypothesis 1. The results for the primitive-number 12 and 20 are just minor variations in the experiments which are most likely caused by the data randomness. We think it is because when the number of primitives increases, the lines in the line drawings becomes denser; therefore it is more difficult

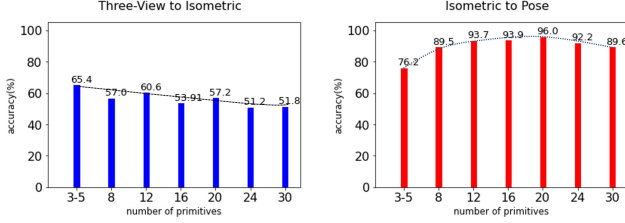


Figure 3. CAD model complexity vs. test accuracy.

for a network to distinguish the tiny difference between candidate line drawings (see the exemplar candidate answers in Figure 1). Thus, we call *T2I* the *detail-hurt* task.

However, unexpected results are shown in Figure 3 right, where the accuracy increases first and then decreases after the primitive number becomes more than 20. We believe it is because, within a certain range of CAD complexity, the more primitives the CAD model contains, the more visual features a network can extract for camera-pose reasoning, thus the higher testing accuracy. However, if a CAD model is too complex, the line drawings become too crowded to provide effective feature extraction and reasoning.

We then notice that the CAD models in the SPARE3D-ABC dataset are mostly from the real world, and their complexity level is close to the CSG models with typically less than 20 primitives. Therefore, for SPARE3D-ABC dataset, we think more shape details can help a network in camera-pose reasoning, which we call a *detail-help* task.

Heuristics 1: the experiment results show our hypothesis is not completely correct. Indeed, more shape details help the camera-pose tasks on the SPARE3D-ABC dataset but hurt the view-consistency task. Therefore, *we may need different methods for them respectively, and an effective method for T2I task should be detail-sensitive to capture detailed differences between candidate answers.*

3.2. Network capacity

Motivation: we want to study if the network’s capacity will affect the baseline performance for tasks on SPARE3D-ABC. Using a large (over-parameterized) network is widely used to achieve better performance on some deep learning tasks [18, 35]. To increase a network’s capacity, we can make the network deeper or wider, without making changes to other components in the network.

Hypothesis 2: *a baseline network’s performance will improve if the network’s capacity increases.*

Experiment details. With the VGG-16 network as a backbone, we define *the width of the network* as the width of the last convolutional layer (the number of output channels). By this definition, the width of the VGG-16 network in [13] is 512. In the comparative experiments, we change the width to 384, 448, and 1024. The width of other convolutional layers is proportionally adapted to the final convolutional layer’s width, ensuring the network’s widths are

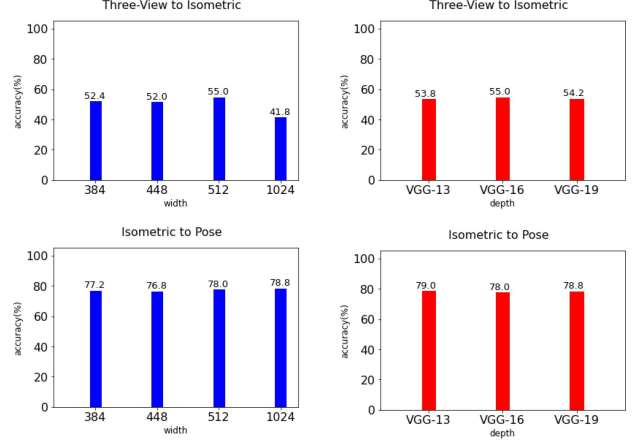


Figure 4. Network capacity (width and depth) vs. test accuracy. The results show that naively increasing the network capacity cannot improve the network performance on *T2I* and *I2P* tasks.

changed gradually. Detailed widths of each layer for the VGG-16 backbone network with different widths can be found in the supplementary. *The depth of the network* represents the number of layers of the VGG family backbone networks. We use VGG-13, VGG-19 based backbone as in [34] to represent three different depths of the network.

Experiment results. For task *T2I*, decreasing the network’s width does not hurt the network’s performance, although strangely, increasing the network’s width leads to a decrease of the testing accuracy (Figure 4 top-left). We think it is because the network with more parameters requires more data, and using the same amount of data to train networks with different widths is insufficient. For the depth control experiments, we find almost no differences among the three selected network depth values (Figure 4 top-right). For task *I2P*, neither the width nor the depth of the network can significantly improve the network’s performance (Figure 4 bottom).

Heuristics 2: our hypothesis is incorrect. In fact, merely increasing network capacities cannot improve the baseline’s performances. Therefore, *to improve SPARE3D performance, we need new networks or losses than only supervised classification networks with larger capacities.*

3.3. Network structure

Motivation: we want to study if the network’s structure can affect the baseline performance for tasks on SPARE3D-ABC. Changing the structure of the network is a potential way to improve the accuracy of some deep learning tasks, e.g., one famous example is to use the residual links in deep networks [15]. To find a proper structure for the view-consistency reasoning task (*T2I*) and camera-pose reasoning tasks (*I2P* and *P2I*), we tried a lot of variants of the backbone network (all variants and the corresponding re-

sults will be shown in supplementary). We also test whether the network’s performance will change if using the pre-trained parameters on Imagenet [8], inspired by [10].

Hypothesis 3: *for each SPARE3D task, a baseline network’s performance will improve if we find a more proper network structure and parameter initialization.*

Experiment details. We find two changes on the network that will have a consistent impact on the network’s performance for all SPARE3D tasks: one is whether the network’s parameters are initialized using Imagenet pre-trained parameters; another one is whether the three-view drawings (front view, right view, and top view drawings) and isometric drawings are fed to separate and independent branches of the network. We call the second one *late fusion*.

Early fusion vs. late fusion. In the original SPARE3D paper [13], the baseline backbone network treats all the input images (front, right, top view drawings, and one isometric view drawing from the candidate answers) as a whole, and it concatenates those images before sending them to the first convolutional layer. We call this way of feeding multi-view line drawings to a network as the *early fusion*. In contrast, we design a network that takes the three-view drawings and the isometric view drawing as separate inputs, which means the input drawings are sent to a convolutional network that shares the *same architecture* yet has *separate network parameters*. We name this way of separately handling the input as the *late fusion* since the extracted image features are concatenated later. Other network structures are kept the same as the baseline method in [13]. Therefore, we have four experiments, which are the combination of training the network with/without Imagenet pre-trained parameters and using *early fusion* or *late fusion*.

For the *P2I* task, we make an extra modification of the network in the baseline method. In the original baseline method, after extracting the input images’ feature vector, the feature vector is concatenated with an 8-dimensional one-hot camera-pose code. Then the concatenated vector is sent to a fully connected layer to obtain a classification probability distribution. Differently, our method extracts the feature of the composite images (F, R, T, and a candidate isometric view image) into an 8-dimensional vector as the camera-pose probability logits of the candidate isometric view. Then we select the logit corresponding to the given pose to compute the cross-entropy loss. We find this minor modification can effectively improve the network’s performance on the *P2I* task. The modification details will be given in the supplementary.

Experiment results. As shown in Table 1, we find that using pre-trained parameters and the *late fusion* can improve the network’s performance on camera-pose reasoning tasks (*I2P* and *P2I*). By using these tactics, the accuracy of *I2P* and *P2I* achieves 85.4% and 72.4% respectively, which is already higher than the baseline in SPARE3D. However,

pre-train	late fusion	<i>T2I</i>	<i>I2P</i>	<i>P2I</i>
n	n	55.0	78.0	64.0
n	y	22.8	80.0	66.6
y	n	30.6	80.4	68.6
y	y	25.2	85.4	72.4

Table 1. **Network architecture vs. performance.** We test four conditions, considering 1) using Imagenet pre-trained parameters or not, 2) using *late fusion method* or *early fusion method*. “y/n” indicates using the network structure or not. *P2I* task uses the slightly improved network structure as previously explained.

the same tactics turned out to decrease the network’s performance on *T2I* task significantly. We leave this puzzling results for our future investigations.

Heuristics 3: based on above results, we believe: 1) *a proper parameter initialization can improve baseline performances*; 2) *using late fusion or early fusion will affect baseline performances, yet the impact depends on the task*. Therefore, for task *T2I*, whose baseline performance is relatively lower than *I2P* and *P2I* (see row 1 of Table 1), we still need a better method. In the next section, we will design a specialized contrastive learning method using all the above heuristics to improve the SPARE3D *T2I* baseline.

4. Contrastive Spatial Reasoning

According to the previous investigation on network architecture, we find that using ImageNet pre-trained parameters to initialize the backbone network will affect the accuracy of all reasoning tasks. Based on this observation, we further explore self-supervised learning to improve the pre-trained parameters. Since the network’s performance on *I2P* and *P2I* are relatively higher than on *T2I*, in this section, we focus on designing a contrastive spatial reasoning method to help the network solve the *T2I* task.

Based on the investigation of Hypothesis 1, *T2I* is a *detail-hurt task*, which means the more complex the models are, the poorer performance the network will have. Therefore, we believe *the key to answering a T2I question is to find an effective way to capture the tiny difference among all the candidate isometric line drawings*, which will help correctly select the isometric drawings that is consistent with the three-view line drawings in the question.

According to the discussion in the Introduction, we believe contrastive learning can help the network learn better line drawing representations. Based on and the previous heuristics and the assumption that it is not difficult to obtain a large number of unlabeled CAD models, we design our specialized contrastive spatial reasoning method (as illustrated in Figure 5). Our method can be divided into three steps: 3D model augmentation; line-drawing feature extraction; contrastive loss computation.

Step 1: 3D data augmentation. Our data augmentation happens in 3D instead of 2D. Then we generate two sets of images: a branch 1 set and a branch 2 set for each

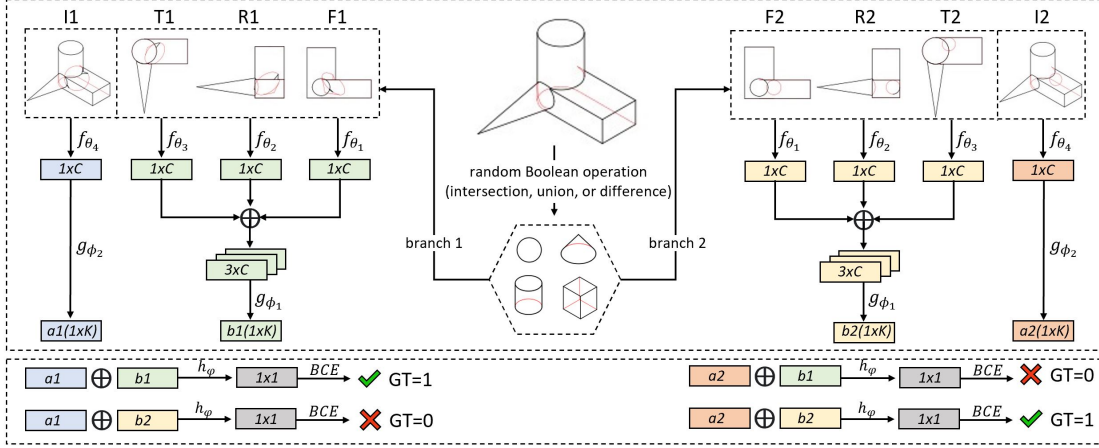


Figure 5. **Contrastive spatial reasoning architecture overview.** A CAD model is used to generate two CAD models with different Boolean operations and primitives like sphere, cone, cylinder, or cube. Then two sets of multi-view line drawings for the two new models are rendered respectively, in branch 1 and 2. Each set is composed of three-view line drawings including Front (F), Right (R), Top (T) line drawings and an isometric (I) line drawing. The a_1, b_1, a_2, b_2 are the encoded feature vectors; C, K are the dimension of the latent vectors. The $f_{\theta_1}, f_{\theta_2}, f_{\theta_3}$, and f_{θ_4} are CNN networks sharing the *same architecture* but with *different parameters*; g_{ϕ_1} and g_{ϕ_2} are three layer MLP sharing the *same architecture* but with *different parameters*; h_{ψ} is a one layer MLP network. \oplus is a concatenation operation. BCE represents binary cross-entropy loss.

augmented CAD model. Each image set contains the three-view drawings and the isometric view drawing. We denote the branch 1 set by $\{F_1, R_1, T_1, I_1\}$, and the branch 2 set by $\{F_2, R_2, T_2, I_2\}$, where F, R, T , and I stand for front, right, top views and the isometric view separately. The branch 1 and branch 2 image sets are generated from two different modifications to the original CAD model. Each modification is a random Boolean operation (intersection, union or difference) on the original CAD model with a random primitive (sphere, cube, cone, or cylinder.) Figure 5 gives an example of generating the two image sets.

Step 2: line-drawing feature extraction. In this paper, f, g, h represent neural networks; θ, ϕ, ψ are the network weights in the three networks respectively. F_i, R_i, T_i , and I_i ($i \in \{1, 2\}$) are fed into four convolutional neural networks (CNN) individually. The four networks are denoted by $f_{\theta_1}, f_{\theta_2}, f_{\theta_3}$, and f_{θ_4} , where $f_{\theta_j} : \mathbb{R}^{3 \times H \times W} \rightarrow \mathbb{R}^C, j \in \{1, 2, 3, 4\}$; H and W are the height and width of the images. Note that the four networks share the *same architecture* but with *different parameters*. Then, the outputs from $f_{\theta_1}, f_{\theta_2}$, and f_{θ_3} are concatenated and fed into a three-layer MLP $g_{\phi_1} : \mathbb{R}^{3C} \rightarrow \mathbb{R}^K$, and the output from f_{θ_4} is fed into another three-layer MLP $g_{\phi_2} : \mathbb{R}^C \rightarrow \mathbb{R}^K$. g_{ϕ_1}, g_{ϕ_2} also share the *same architecture* but with *different parameters*. The outputs from g_{ϕ_1} and g_{ϕ_2} are noted as a_i and b_i ($i \in \{1, 2\}$), which encode the information from the 3-view images and the isometric image respectively.

Step 3: Contrastive loss computation. After having the four latent codes (a_1, a_2, b_1 , and b_2), we concatenate each a and each b , which gives four combinations $a_1 \oplus b_1$, $a_1 \oplus b_2$, $a_2 \oplus b_1$, and $a_2 \oplus b_2$ (see Figure 5). Then we send the four concatenated latent codes to a binary classi-

fier $h_{\psi} : \mathbb{R}^{2K} \rightarrow (0, 1)$, where the h_{ψ} is an MLP. The outputs from h_{ψ} are $\hat{p}_1, \hat{p}_2, \hat{p}_3$, and \hat{p}_4 respectively, and are used to compute the binary cross entropy (BCE) loss with the ground truth. We define the ground truth to be 1 if the original two latent codes used to concatenate are from the same image pairs, and the ground truth to be 0 from different image pairs. Therefore, $p_1 = p_4 = 1, p_2 = p_3 = 0$. The final loss is $\frac{1}{4} \sum_{k=1}^4 BCE(\hat{p}_k, p_k), (k \in \{1, 2, 3, 4\})$.

We notice that all the learned parameters θ, ϕ, ψ can be loaded to the neural network for further supervised fine-tuning, because the contrastive spatial reasoning method is just a pre-training step and it uses exactly the same network architecture as the network for the supervised learning.

Difference with SimCLR. Unlike existing contrastive learning methods such as SimCLR, the representation from our method are designed to be both multi-view-consistent and detail-sensitive. Technically, our method differs from them in that: 1) our data augmentation operates on 3D CAD models with Boolean operations (intersection, union, or difference), instead of single-image operations like random cropping, color distortion, and Gaussian blur; 2) our positive pairs are two sets of multi-view line drawings (three-view line drawings and isometric line drawing) that are rendered in the same data branch, and our negative pairs are image sets from different data branches, unlike being sampled from other data instances; 3) we use binary cross-entropy loss to optimize the network, unlike the NT-Xent loss which has the temperature parameter to tune.

5. Experiment

In this section, we compare classification accuracy of our method with other methods on the $T2I$ task. We also visu-

Supervised learning (5K)	14K	Jigsaw puzzle[29]	Colorization[44]	SimCLR[6]	Ours (direct)	Ours (fine-tuned)
25.2/30.6/55.0	27.4/51.4/63.6	27.4/54.8/-	23.4/30.6/-	31.0/-/-	71.4/-/-	74.9/-/-

Table 2. **Comparison of performance on $T2I$ for different methods.** The accuracy number a/b/c in the table for each method means: (a) using *late fusion method* with pre-trained parameters for supervised learning, (b) using *early fusion method* with pre-trained parameters for supervised learning, (c) using *early fusion method* with no pre-trained parameters for supervised learning. For SimCLR and our methods, the supervised learning network cannot be designed as early fusion, since it requires two branches for loss computation. 5K and 14K means the total number of data used for training and testing.

alize the attention maps obtained from our methods and supervised baseline methods, demonstrating that our method can better localize the differences between the candidate answers. We also conduct ablation studies to test the most suitable settings for our method. All experiments are implemented with PyTorch [30], using NVIDIA GeForce GTX 1080 Ti GPU.

Data for training and testing. As mentioned in our contrastive learning approach, we need to generate image sets first. In practice, we download 14,051 models from the ABC dataset for training, and 737 models for testing. Then we use PythonOCC [31] to implement two random Boolean operations on each model for branch 1 and branch 2 image sets generation. Therefore, we have $14,051 \times 8$ rendered images. These images are also used for two self-supervised baselines that we compare with, namely Jigsaw Puzzle and Colorization. For SimCLR, we use all the branch 1 image sets, which contains $14,051 \times 4$ images. For supervised-learning with 5K dataset, we use the original data from SPARE3D paper, with 5,000 questions. For supervised learning with 14K dataset, we use the 14,051 CAD models to generate new questions for training.

We avoid using the same models for self-supervised training and supervised fine-tuning. In practice, all the 14,051 models have different model indices from the model indices in the 5,000 questions with ground truth labels.

Hyperparameter settings. For our contrastive spatial reasoning network, we find that the learning rate 0.00005 and batch size 4 can achieve the best performance. We find that the learning rate 0.00001 achieves the best performance in all other tasks, including self-supervised learning tasks and supervised learning tasks. The batch size for Jigsaw puzzle, SimCLR, and Colorization are 10, 30, 70, respectively. For supervised learning tasks, we find that batch size equal to 3 and 16 works the best for the *late fusion method* and *early fusion method*, respectively.

Details of our network. For our method, we use VGG-16 network as the backbone for image feature extraction. The size of input line drawings are $200 \times 200 \times 3$. The output of the last convolutional layer is a $6 \times 6 \times 512$ feature map. The value of C is set to be 18,432 (by flattening the $6 \times 6 \times 512$ feature map). The value of K is set to be 4096, same as in the SPARE3D paper.

Baseline network adaptation. All the methods used to compare with our method in Table 2 are implemented us-

ing the original papers’ network designs. However, to adapt these baseline methods to the SPARE3D tasks, we change all the backbone networks to VGG-16 to ensure that the learned parameters can be loaded to our supervised training network. For SimCLR, we define the positive image pairs in our case as the F , R , T and I images which are generated from the same CAD model. We use the *late fusion* structure to handle input images individually. Then, the learned parameters $\theta_1, \theta_2, \theta_3, \theta_4, \phi_1, \phi_2, \psi$ can be loaded for supervised fine-tuning with the *late fusion*. For Jigsaw puzzle and Colorization, the VGG-16 backbone network takes one single image as the input. Therefore, on the one hand, we can load the learned parameters θ for supervised fine-tuning with the *early fusion*, discarding the first convolutional layer’s parameters. On the other hand, we can load the learned parameters θ for supervised fine-tuning with the *late fusion*, by initializing the parameters of the four f networks with the same pre-trained parameters.

5.1. Quantitative results

Classification accuracy. As can be seen in Table 2, our methods (both with or without fine-tuning) outperform other methods. Our fine-tuned result can achieve 74.9% accuracy on $T2I$ task, approaching the average untrained human performance of 80.5%.

We believe the good performance of our method is because contrastive learning helps the network learn the *detail-sensitive* yet view-invariant visual representations in the line drawings. This reason could also explain an interesting phenomenon that we observe, which is that the direct evaluation (without fine-tuning) using the learned parameters from contrastive spatial reasoning can achieve 71.4% accuracy (see Table 2). Thus, a good visual representation should be able to transfer to the downstream tasks with little further training.

Although we use more data in the contrastive pre-training, the higher accuracy of our method is not only due to increased data volume. As aforementioned, we use 14,051 CAD models to generate image sets for contrastive learning. We also use these models to generate 14,051 questions for purely supervised learning. This ensures the number of CAD models used for our method is the same as for purely supervised learning. With the same number of CAD models for training (14K dataset), we find the best performance that the purely supervised learning can achieve

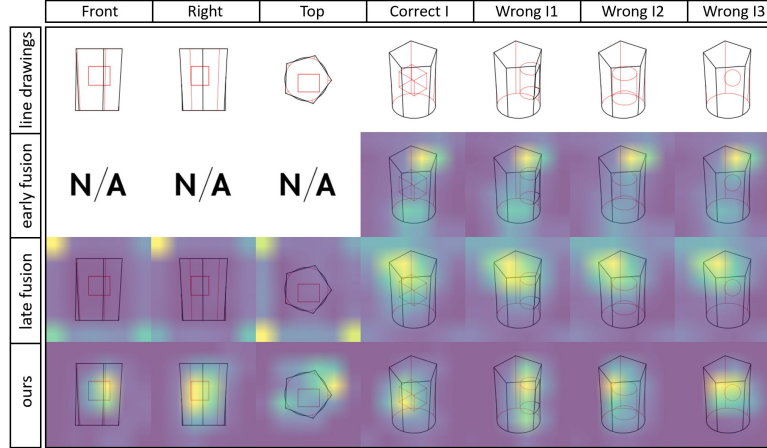


Figure 6. **Attention maps for our method vs. supervised learning.** For each CAD model, the first row are the line drawings. The second and third row are the attention maps generated from supervised learning using *early fusion* and *late fusion*, respectively. The fourth row are the attention maps generated from our method. N/A indicates no attention map for the corresponding view. Best viewed in color.

is 63.6%, which uses the *early fusion* with no pre-trained parameters. Although increasing the data volume can help improve the baseline performance for supervised learning, from 55.0% to 63.6%, the result is still significantly lower than our method, which is 74.9%.

Imagenet pre-training helps contrastive spatial reasoning network converge. We find it a necessity to use the Imagenet pre-trained parameters to initialize the VGG-16 network for our method, otherwise it cannot converge. Without the pre-trained parameters, the training and testing accuracy of contrastive learning is around 25%, showing the network solves the problem using random guesses. It coincides with the conclusion from the controlled experiment that Imagenet pre-training has influence on the network’s performance. It seems that although these learned parameters are pre-trained on Imagenet dataset for image classification problem, which is a different domain of solving spatial reasoning tasks using line drawings, they can still help contrastive learning.

5.2. Qualitative results

We visualize the attention map for our method and supervised learning method using the schemes in [41]. For supervised learning, we generate attention maps on both *early fusion* and *late fusion* method with no pre-trained parameters. For *early fusion*, the input line drawings, including front, right, top, and one isometric line drawing are concatenated before being sent to the CNN. Therefore, for each composite image, it will have one attention map. We put the attention map with the corresponding candidate isometric line drawing, leaving the attention map for front, right, and top as empty. For *late fusion* and our method, after having the attention map for each input image, we put it together with the corresponding input line drawing. All the results are shown in Figure 6 (more results in the supplementary). The

backbone	VGG-13	VGG-16	VGG-19
acc	72.0	74.9	75.0

Table 3. **Comparison of using different VGG backbones.** The results show that VGG-19 is most suitable for our method.

comparison between the three rows of attention maps generated from the three methods shows that our method can help the CNN better capture the tiny detailed differences between the candidate answer drawings, which is the key to select the correct answer from four similar options.

We also explore the best VGG network as the backbone for our method. As can be seen from Table 3, we find VGG-19 can provide the best performance among three different types of VGG network.

6. Conclusion

We conduct three controlled experiments to explore the factors that might affect baseline performance. We find that 1) merely increasing the capacity of the network cannot improve the performance; 2) network structure will affect the performance; 3) different tasks need different methods, and for task *T2I*, the method must be detail-sensitive yet view-invariant. Based on these hindsight, we propose a simple yet effective contrastive learning method for line drawings in SPARE3D. More specifically, our method outperforms the prior method in SPARE3D by a large margin, and it shows more reasonable attention maps. We conjecture that our method is effective because it can effectively learn detail-sensitive yet view-invariant representations.

Acknowledgment

The research is supported by NSF Future Manufacturing program under EEC-2036870. Siyuan Xiang gratefully thanks the IDC Foundation for its scholarship. We also thank the anonymous reviewers for constructive feedback.

References

- [1] Ankesh Anand. Contrastive self-supervised learning, 2020. <https://ankeshanand.com/blog/2020/01/26/contrastive-self-supervised-learning.html>. 2
- [2] Sanjeev Arora, Hrishikesh Khandeparkar, Mikhail Khodak, Orestis Plevrakis, and Nikunj Saunshi. A theoretical analysis of contrastive unsupervised representation learning. *arXiv preprint arXiv:1902.09229*, 2019. 2
- [3] Philip Bachman, R Devon Hjelm, and William Buchwalter. Learning representations by maximizing mutual information across views. In *Advances in Neural Information Processing Systems*, pages 15535–15545, 2019. 2
- [4] Yoshua Bengio. The consciousness prior. *arXiv preprint arXiv:1709.08568*, 2017. 2
- [5] Mathilde Caron, Ishan Misra, Julien Mairal, Priya Goyal, Piotr Bojanowski, and Armand Joulin. Unsupervised learning of visual features by contrasting cluster assignments. *Advances in Neural Information Processing Systems*, 33, 2020. 2
- [6] Ting Chen, Simon Kornblith, Mohammad Norouzi, and Geoffrey Hinton. A simple framework for contrastive learning of visual representations. *arXiv preprint arXiv:2002.05709*, 2020. 2, 7
- [7] Ting Chen, Simon Kornblith, Kevin Swersky, Mohammad Norouzi, and Geoffrey E Hinton. Big self-supervised models are strong semi-supervised learners. *Advances in Neural Information Processing Systems*, 33, 2020. 2
- [8] Jia Deng, Wei Dong, Richard Socher, Li-Jia Li, Kai Li, and Li Fei-Fei. Imagenet: A large-scale hierarchical image database. In *Proceedings of the IEEE Conference on Computer Vision and Pattern Recognition*, pages 248–255. Ieee, 2009. 2, 5
- [9] Carl Doersch, Abhinav Gupta, and Alexei A Efros. Unsupervised visual representation learning by context prediction. In *Proceedings of the IEEE international conference on computer vision*, pages 1422–1430, 2015. 2
- [10] Christina M Funke, Judy Borowski, Karolina Stosio, Wieland Brendel, Thomas SA Wallis, and Matthias Bethge. The notorious difficulty of comparing human and machine perception. *arXiv preprint arXiv:2004.09406*, 2020. 3, 5
- [11] Spyros Gidaris, Praveer Singh, and Nikos Komodakis. Unsupervised representation learning by predicting image rotations. *arXiv preprint arXiv:1803.07728*, 2018. 2
- [12] Clément Godard, Oisín Mac Aodha, Michael Firman, and Gabriel J Brostow. Digging into self-supervised monocular depth estimation. In *Proceedings of the IEEE international conference on computer vision*, pages 3828–3838, 2019. 2
- [13] Wenyu Han, Siyuan Xiang, Chenhui Liu, Ruoyu Wang, and Chen Feng. Spare3d: A dataset for spatial reasoning on three-view line drawings. In *Proceedings of the IEEE Conference on Computer Vision and Pattern Recognition*, pages 14690–14699, 2020. 1, 3, 4, 5
- [14] Kaiming He, Haoqi Fan, Yuxin Wu, Saining Xie, and Ross Girshick. Momentum contrast for unsupervised visual representation learning. In *Proceedings of the IEEE Conference on Computer Vision and Pattern Recognition*, pages 9729–9738, 2020. 2
- [15] Kaiming He, Xiangyu Zhang, Shaoqing Ren, and Jian Sun. Deep residual learning for image recognition. In *Proceedings of the IEEE Conference on Computer Vision and Pattern Recognition*, pages 770–778, 2016. 3, 4
- [16] R Devon Hjelm, Alex Fedorov, Samuel Lavoie-Marchildon, Karan Grewal, Phil Bachman, Adam Trischler, and Yoshua Bengio. Learning deep representations by mutual information estimation and maximization. *arXiv preprint arXiv:1808.06670*, 2018. 2
- [17] Sherry Hsi, Marcia C Linn, and John E Bell. The role of spatial reasoning in engineering and the design of spatial instruction. *Journal of engineering education*, 86(2):151–158, 1997. 1
- [18] Yanping Huang, Youlong Cheng, Ankur Bapna, Orhan Firat, Dehao Chen, Mia Chen, HyukJoong Lee, Jiquan Ngiam, Quoc V Le, Yonghui Wu, et al. Gpipe: Efficient training of giant neural networks using pipeline parallelism. In *Advances in Neural Information Processing Systems*, pages 103–112, 2019. 3, 4
- [19] Daniel Kahneman. *Thinking, fast and slow*. Macmillan, 2011. 2
- [20] Harrison J Kell, David Lubinski, Camilla P Benbow, and James H Steiger. Creativity and technical innovation: Spatial ability’s unique role. *Psychological science*, 24(9):1831–1836, 2013. 1
- [21] Dahun Kim, Donghyeon Cho, Donggeun Yoo, and In So Kweon. Learning image representations by completing damaged jigsaw puzzles. In *2018 IEEE Winter Conference on Applications of Computer Vision (WACV)*, pages 793–802. IEEE, 2018. 2
- [22] Ildoo Kim, Woonhyuk Baek, and Sungwoong Kim. Spatially attentive output layer for image classification. In *Proceedings of the IEEE Conference on Computer Vision and Pattern Recognition*, pages 9533–9542, 2020. 2
- [23] Youngsung Kim, Jinwoo Shin, Eunho Yang, and Sung Ju Hwang. Few-shot visual reasoning with meta-analogical contrastive learning. *Advances in Neural Information Processing Systems*, 33, 2020. 3
- [24] Gustav Larsson, Michael Maire, and Gregory Shakhnarovich. Learning representations for automatic colorization. In *European Conference on Computer Vision*, pages 577–593. Springer, 2016. 2
- [25] Jason D Lee, Qi Lei, Nikunj Saunshi, and Jiacheng Zhuo. Predicting what you already know helps: Provable self-supervised learning. *arXiv preprint arXiv:2008.01064*, 2020. 2
- [26] Xiao Liu, Fanjin Zhang, Zhenyu Hou, Zhaoyu Wang, Li Mian, Jing Zhang, and Jie Tang. Self-supervised learning: Generative or contrastive. *arXiv preprint arXiv:2006.08218*, 2020. 2
- [27] Ishan Misra and Laurens van der Maaten. Self-supervised learning of pretext-invariant representations. In *Proceedings of the IEEE Conference on Computer Vision and Pattern Recognition*, pages 6707–6717, 2020. 2
- [28] Paul Murty, Scott Chase, and Joseph Nappa. Evaluating the complexity of cad models in education and practice. 1999. 3
- [29] Mehdi Noroozi and Paolo Favaro. Unsupervised learning of visual representations by solving jigsaw puzzles. In *European Conference on Computer Vision*, pages 69–84. Springer, 2016. 2, 7

- [30] Adam Paszke, Sam Gross, Francisco Massa, Adam Lerer, James Bradbury, Gregory Chanan, Trevor Killeen, Zeming Lin, Natalia Gimelshein, Luca Antiga, Alban Desmaison, Andreas Kopf, Edward Yang, Zachary DeVito, Martin Raison, Alykhan Tejani, Sasank Chilamkurthy, Benoit Steiner, Lu Fang, Junjie Bai, and Soumith Chintala. PyTorch: An imperative style, high-performance deep learning library. In *Advances in Neural Information Processing Systems*, pages 8024–8035, 2019. 3, 7
- [31] PythonOCC. 3D CAD/CAE/PLM development framework for the Python programming language, 2018. <http://www.pythonocc.org>. 7
- [32] Ajay Ramful, Thomas Lowrie, and Tracy Logan. Measurement of spatial ability: Construction and validation of the spatial reasoning instrument for middle school students. *Journal of Psychoeducational Assessment*, 35(7):709–727, 2017. 1
- [33] Jürgen Riegel, Werner Mayer, and Yorik van Havre. Freecad, 2016. 3
- [34] Karen Simonyan and Andrew Zisserman. Very deep convolutional networks for large-scale image recognition. *arXiv preprint arXiv:1409.1556*, 2014. 3, 4
- [35] Mingxing Tan and Quoc V Le. Efficientnet: Rethinking model scaling for convolutional neural networks. *arXiv preprint arXiv:1905.11946*, 2019. 3, 4
- [36] Yonglong Tian, Dilip Krishnan, and Phillip Isola. Contrastive multiview coding. *arXiv preprint arXiv:1906.05849*, 2019. 3
- [37] Yuandong Tian, Lantao Yu, Xinlei Chen, and Surya Ganguli. Understanding self-supervised learning with dual deep networks. *arXiv preprint arXiv:2010.00578*, 2020. 2
- [38] Christopher Tosh, Akshay Krishnamurthy, and Daniel Hsu. Contrastive learning, multi-view redundancy, and linear models. *arXiv preprint arXiv:2008.10150*, 2020. 2
- [39] Yude Wang, Jie Zhang, Meina Kan, Shiguang Shan, and Xilin Chen. Self-supervised equivariant attention mechanism for weakly supervised semantic segmentation. In *Proceedings of the IEEE Conference on Computer Vision and Pattern Recognition*, pages 12275–12284, 2020. 2
- [40] Chen Wei, Lingxi Xie, Xutong Ren, Yingda Xia, Chi Su, Jiaying Liu, Qi Tian, and Alan L Yuille. Iterative reorganization with weak spatial constraints: Solving arbitrary jigsaw puzzles for unsupervised representation learning. In *Proceedings of the IEEE Conference on Computer Vision and Pattern Recognition*, pages 1910–1919, 2019. 2
- [41] Sergey Zagoruyko and Nikos Komodakis. Paying more attention to attention: Improving the performance of convolutional neural networks via attention transfer. *arXiv preprint arXiv:1612.03928*, 2016. 8
- [42] Sergey Zagoruyko and Nikos Komodakis. Wide residual networks. *arXiv preprint arXiv:1605.07146*, 2016. 3
- [43] Chi Zhang, Feng Gao, Baoxiong Jia, Yixin Zhu, and Song-Chun Zhu. Raven: A dataset for relational and analogical visual reasoning. In *Proceedings of the IEEE Conference on Computer Vision and Pattern Recognition*, pages 5317–5327, 2019. 3
- [44] Richard Zhang, Phillip Isola, and Alexei A Efros. Colorful image colorization. In *European Conference on Computer Vision*, pages 649–666. Springer, 2016. 2, 7

Appendix

A. Details for Controlled Experiments

Controlled experiment hyperparameter settings. For all our controlled experiments, we run each experiment for 5 times and select the best result as the final result. Specifically, for controlled experiments investigating *CAD model complexity* factor, we tune the learning rate as 0.00001 and batch size as 16 to achieve the best performance for all the dataset with the different number of primitives on task *T2I* and *I2P*. For controlled experiments investigating *network capacity (width and depth)* factor, we tune the learning rate as 0.00001 and batch size as 6 to achieve the best performance for *T2I* task. For the *I2P* task, the learning rate is 0.00005 and batch size is 70. For controlled experiments investigating *network structure* factor, we tune the learning rate as 0.00001 and batch size as 16 to achieve the best performance for all modified baseline networks on *T2I* task. For the *I2P* task, the most suitable learning rate is 0.00005, and the most suitable batch size is 50. For *P2I* task, the learning rate is tuned to be 0.00005, and the batch size is tuned to be 16.

Network width for *T2I* and *I2P* tasks. Network width is the factor that investigated in the section 3.2. Table 4 shows the detailed network width for all VGG-16 based backbone network with different widths, for *T2I* and *I2P* tasks.

	384	448	512	1024
1 – 2	48	56	64	128
3 – 4	96	112	128	256
5 – 7	192	224	256	512
8 – 13	384	448	512	1024

Table 4. **Network width for VGG-16 based backbone network.** 384, 448, 512, 1024 are the width of the modified VGG-16 backbone network. 1 – 2, 3 – 4, 5 – 7, 8 – 13 means convolutional layer 1 – 2, 3 – 4, 5 – 7, 8 – 13 respectively. The number in each cell means the width of that convolutional layer (the number of channels).

Network structure for *P2I* task. As aforementioned, we modify the baseline method for the *P2I* task. In this section, we will introduce the details of the modified method for the *P2I* task.

Each question in *P2I* task contains the 3-view(front, right, top view) line drawings and one given pose out of eight views. We note these three drawings as F, R, T , and the given pose as P_m , ($m \in \{1, 2, 3, 4, 5, 6, 7, 8\}$). The answers provide four candidate drawings. These candidate drawings are isometric view line drawings rendered from four views, which are randomly selected from eight views designed in SPARE3D dataset. We note the four candidate answers as I_1, I_2, I_3, I_4 . For the *early fusion method*, we concatenate F, R, T and one of the isometric drawings I_i , ($i \in \{1, 2, 3, 4\}$) to form a 12 – channel composite image I_{c_i} , ($i \in \{1, 2, 3, 4\}$). Then, we send I_{c_i} to a VGG-based classifier: $g_\theta : \mathbb{R}^{12 \times H \times W} \rightarrow \mathbb{R}^8$, where θ represents the parameters in the network. The 8 number codeword represents the probability of the composed image I_{c_i} belonging to eight coded views. Then, we pick the number of the codeword corresponding to view

the P_m , note as \hat{p}_{m_i} , ($i \in \{1, 2, 3, 4\}$). The ground truth is set to be 1 if the candidate isometric drawing is rendered from view P_m , and otherwise 0. With the provided ground truth p_m , we can compute the BCE loss to train the neural network, which is: $\frac{1}{4} \sum_{k=1}^4 BCE(\hat{p}_{m_k}, p_{m_k})$.

Network structure for all tasks. As we mentioned in the previous section, we change many variants of the baseline network for three tasks, to see if a variant will affect the network’s performance on the task. Here, we list out all the variants we tried and the results. Among them, two changes have a consistent impact on three tasks, which are already explained and discussed in the previous section. Therefore, we will talk about other variants, which do not have an obvious influence on the network’s performance.

As can be seen in Table 5, we provide six variants, with two factors (“pre-train” and “late fusion”) discussed in the previous section. We will focus on the remaining four variants, which are “no pooling”, “no dropout”, “share weight”, “separate fc” respectively. “no pooling” means we discard all the adaptive average pooling layer in the VGG-16 backbone. “no dropout” means we delete all the dropout layers in the VGG-16 backbone. “share weight” means for the *late fusion method*, all the VGG-16 backbone use the *same architecture* and with *same parameters*. “separate fc” means for the *late fusion method*, the front, right, top view drawings are first fed into the VGG-16 backbone based network: $g_\phi : \mathbb{R}^{3 \times H \times W} \rightarrow \mathbb{R}^{18432}$. We note the image features as c_f, c_r, c_t separately. Then we concatenate the three codewords to form a code word, and maps it via an MLP: $g_\psi : \mathbb{R}^{55296} \rightarrow \mathbb{R}^{18432}$. For the isometric drawing, we send it to the VGG-16 backbone based network: $g_\phi : \mathbb{R}^{1 \times H \times W} \rightarrow \mathbb{R}^{18432}$. Finally, we concatenate the two codewords generated from 3-view drawings and isometric drawing as the feature vector for the classification. Other parts of the network are the same as not using the “separate fc” structure.

Table 5 reveals that “no pooling”, “no dropout”, “share weight”, “separate fc” has no obvious and consistent impact on the network’s performance. Since rows with an odd number as index differ from the rows with even numbers in “pre-train”, each time we will compare two odd rows, which are not using “pre-train”. The same conclusion can be drawn if we compare two even rows each time.

We can compare the 1 row with the 3 row, and we can find that “no pooling” does not obviously affect the results. If we compare the 1 row with the 5 row, we can find “no dropout” also cannot help the network perform better. Comparing the 1 row with the 7 row, we have the conclusion that using both “no pooling” and “no dropout” could not improve the network’s classification accuracy.

For 9, 11, 13 rows, we use the *late fusion method*. Based on this method, we vary the network’s structure of the remaining four variants. We also find these four variants do not have a significant influence on the network for *late fusion method*. For 9 row, “no pooling” and “no dropout” seem not to impact on the classification results; for 11 row, “no pooling”, “no dropout”, and “separate fc” does not work; for 13 row, all the four variants cannot help improve the performance.

Therefore, we conclude that except for the two factors we mentioned in the previous section, the other four factors do not have an obvious impact on the final classification results on the *I2P* task.

index	pre-train	late fusion	no pooling	no dropout	share weight	separate fc	max	avg
1	n	n	n	n	n	n	76.8	72.5
2	y	n	n	n	n	n	80.4	78.9
3	n	n	y	n	n	n	76.4	71.1
4	y	n	y	n	n	n	79.4	79.1
5	n	n	n	y	n	n	77.8	69.1
6	y	n	n	y	n	n	81.2	80.9
7	n	n	y	y	n	n	70.4	66.8
8	y	n	y	y	n	n	80.8	79.1
9	n	y	y	y	n	n	78.8	77.4
10	y	y	y	y	n	n	86.4	84.1
11	n	y	y	y	n	y	80.0	76.0
12	y	y	y	y	n	y	85.4	84.3
13	n	y	y	y	y	y	75.6	74.2
14	y	y	y	y	y	y	85.4	84.9

Table 5. **Network architecture vs. performance on *I2P* task.** The backbone used is VGG-16. The rows in the green background represent the networks are not initialized with the Imagenet pre-trained parameter, while the rows in the white background are initialized with the parameters. Every two rows (odd row and even row) can be compared to see the influence of using pre-trained parameters or not. We provide the max and average results for each type of network based on seven times of implementation.

B. Additional Examples of Attention Maps

We provide more visualization results of attention maps to compare our method with supervised learning method, including Figure 7, Figure 8, and Figure 9.

	Front	Right	Top	Correct I	Wrong I1	Wrong I2	Wrong I3
line drawings							
early fusion	N/A	N/A	N/A				
late fusion							
ours							
line drawings							
early fusion	N/A	N/A	N/A				
late fusion							
ours							

Figure 7. Additional attention maps for our method vs. supervised learning.

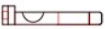


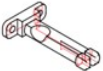
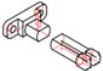
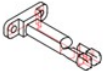
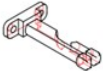

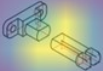
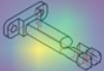
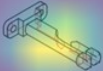

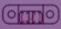

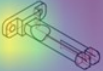
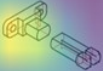
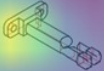
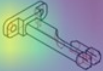


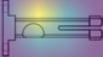
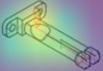
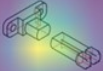
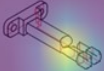
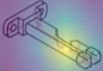

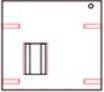

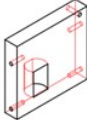

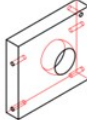


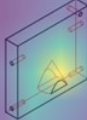

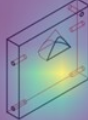




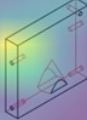



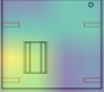





	Front	Right	Top	Correct I	Wrong I1	Wrong I2	Wrong I3
line drawings							
early fusion	N/A	N/A	N/A				
late fusion							
ours							
line drawings							
early fusion	N/A	N/A	N/A				
late fusion							
ours							

Figure 8. Additional attention maps for our method vs. supervised learning.

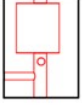
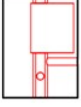

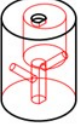
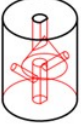
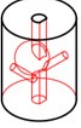





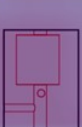
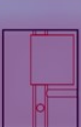













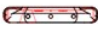














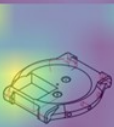





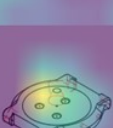
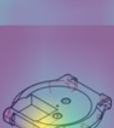
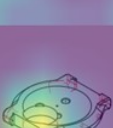
	Front	Right	Top	Correct I	Wrong I1	Wrong I2	Wrong I3
line drawings							
early fusion	N/A	N/A	N/A				
late fusion							
ours							
line drawings							
early fusion	N/A	N/A	N/A				
late fusion							
ours							

Figure 9. Additional attention maps for our method vs. supervised learning.